Electronic Supplementary Material (ESI) for Biomaterials Science.

SUPPLEMENTARY INFORMATION

Nanomedicine targeting brain lipid metabolism as a feasible approach for controlling energy balance

Jesús Garcia-Chica[a†], West Kristian Dizon Paraiso [b†‡], Sebastián Zagmutt[a], Anna Fosch[a], Ana Cristina Reguera[a], Sara Alzina[a], Laura Sánchez-García[a], Shigeto Fukushima[b], Kazuko Toh[b], Núria Casals[a] , Dolors Serra[cd], Laura Herrero[cd], Jordi Garcia[ce], Kazunori Kataoka[b], Xavier Ariza[ce], Sabina Quader[b*] and Rosalía Rodríguez-Rodríguez [ac*]

[a] Basic Sciences Department, Faculty of Medicine and Health Sciences, Universitat Internacional de Catalunya (UIC), Sant Cugat del Vallès, E-08195 Spain.

[b] Innovation Center of Nanomedicine, Kawasaki Institute of Industrial Promotion, Kawasaki, Kanagawa 210-0821 Japan

[c] Centro de Investigación Biomédica en Red de Fisiopatología de la Obesidad y la Nutrición (CIBEROBN), Instituto de Salud Carlos III, Madrid, E-28029 Spain.

[d] Department of Biochemistry and Physiology, School of Pharmacy and Food Sciences, Institut de Biomedicina de la Universitat de Barcelona (IBUB), Universitat de Barcelona, Barcelona, E-08028 Spain.

[e] Department of Inorganic and Organic Chemistry, Faculty of Chemistry, Institut de Biomedicina de la Universitat de Barcelona (IBUB), Universitat de Barcelona (UB), Barcelona, E-08028 Spain.

***Corresponding authors: Rosalía Rodríguez-Rodríguez (rrodriguez@uic.es) (Tel. +34-935-042-002) and Sabina Quader (sabina-q@kawasaki-net.ne.jp) (Tel. +81-44-589-5920)**

† Equal contribution.

‡ Present address: Red Arrow Therapeutics Co., Ltd., Tokyo 113-0033 Japan

EXPERIMENTAL SECTION

Characterization of micelles

For DLS measurements (Zetasizer Ultra, Malvern Panalytical, Spectris plc, UK), PM suspensions were diluted to 1 mg/mL and placed inside a ZEN2112 quartz cuvette. Light scattering data was measured using a 50-mW 532 nm DPSS laser incident beam at a detection angle of 173° with a He-Ne laser 633 nm (temperature = 25 °C). The autocorrelation function produced was analysed through the cumulant approach. Size is expressed as the hydrodynamic diameter, which was calculated with the Stokes−Einstein equation. Attenuator selection was automated. For zeta potential measurements, micelle suspensions were introduced in a ZEN1010 HC cell, using the Smoluchowski approach.

For quantification of cargo inside the micelles, PM solutions were pipetted into Amicon Ultra-0.5 mL centrifugal filters (MWCO 10,000, Merck Millipore, cat. # UFC501096) and spun (14,000 g, 15 min, 4 °C). The filtrate was then collected, weighed, and then transferred into UV-transparent 96-well plates. Its absorption at λ_{max} CoA = 259 nm was measured using a microplate reader (Infinite® M1000 Pro, Tecan Trading AG, Switzerland). Drug encapsulation was calculated by getting the ratio of the filtrate absorbance to that of the original (±)-C75-CoA solution added to form the PM.

Micelle and polymer morphology was observed on a Transmission Electron Microscope (JEM-2100, JEOL, Japan) operated with 120 kv acceleration voltages and approximately 60 µA beam current. The diluted micelle or polymer solution (0.1 mg/mL) was stained by mixing with uranyl acetate solution (2%, w/v) and placed on 400-mesh copper grids before drying and observation.

Preparation of labelled polymers and FRET micelles

PEG–PBLA–PLys(TFA) (50 mg) was dissolved in anhydrous DMSO (Sigma-Aldrich, cat. # 276855-100ML) to which rhodamine-NHS ester (ThermoFisher Scientific, cat. # 46406:10 eq) was added. The reaction mixture was stirred at 40 °C for 72 h. After which, the labelled polymer was isolated by precipitation and washing in cold ether (3×). After drying *in vacuo*, aminolysis and deprotection were carried out as described in the main text.

PEG–PBLA (50 mg) was dissolved in anhydrous DMSO (Sigma-Aldrich, cat. # 276855-100ML) to which fluorescein-NHS ester (ThermoFisher Scientific, cat. # 46410:10 eq) was added. The reaction mixture was stirred at 40 °C for 72 h. After which, the labelled polymer was isolated by precipitation and washing in cold ether (3×). After drying *in vacuo*, hydrazinolysis was carried out as reported [1].

FRET micelles were prepared with buffered solutions of (±)-C75-CoA as above. FRET behaviour was confirmed by fluorescence spectroscopy (fluorescence spectrometer FP-8600DS, JASCO, Japan), where excitation wavelength 494 nm for fluorescein was used.

Cell culture, cellular uptake, fluorescent assays and ATP measurement

Murine hypothalamic neuronal cells GT1-7 (Merck Millipore, Sigma, Madrid, Spain) were cultured in DMEM (4.5 g/L glucose) as described [2]. For cellular uptake analysis, GT1-7 cells (5×10^4 cells / well) were seeded in 24-well plates 24 h prior to the assay. They were then incubated with PM suspension in medium (micelle amount equivalent to 0.1 mg/mL Fluor-CoA) for 30 min, followed by washing of cell suspension then incubated with 50 µL Accutase® Cell Detachment Solution (Innovative Cell Technologies, San Diego, California) for 3 minutes at 37 °C, centrifuged and resuspended with DAPI, as described [2]. After final washing, the cells were resuspended. Mean fluorescence intensity and percentage of Fluor-CoA+ cells in FITC channel were measured by flow cytometry (BD LSRFortessa™ Flow

Cytometer, BD Biosciences, San Jose, California) using FSC and SSC detection to gate out debris, and the UV (355 nm) and blue lasers (488 nm) for the detection of DAPI and Fluor-CoA, respectively. Data analysis was performed using FlowJo software (BD Biosciences, San Jose, California).

The protocol for ATP measurement was based on previous publication [2]. Briefly, produced ATP was quantified using a luminescence assay. The GT1-7 cells (2×10^5 cells/well) were seeded in a white, flat-bottom 96-well tissue culture plate 24 h prior to the assay. The cells were then incubated with control, free drug, or micelles (0.5 mM) in bicarbonate-free DMEM (Sigma-Aldrich, cat. # D5030-10L) supplemented with 2.5 mM glucose (Gibco, cat. # A2494001) and 275 nM oleate-BSA (Sigma-Aldrich, cat. # O3008-5ML) for 1 h in a separate incubator at 0% CO_2, 20% O_2, 37 °C. The assay was then performed according to manufacturer protocol (CellTiter-Glo® Luminescent Cell Viability Assay, Promega). Luminescence signal for 10 s was measured in each well using GloMax® Multi Detection System (Promega Corp, Madison, Wisconsin).

For colocalization analysis of the nanomedicine with acidic organelles, GT1-7 cells exposed to the polymeric micelle Fluorescein-CoA-PM for 1h at 37°C, were concomitantly incubated with LysoTracker® Red (Thermo Fisher Scientific, Waltham, MA, USA) for endolysosomes staining, and compared to MitoTracker® Red (Thermo Fisher Scientific, Waltham, MA, USA) for staining of mitochondria. Cells were then fixed with 4% paraformaldehyde and counterstained with Hoechst for the nuclei visualization (blue). Images were taken using a Leica TCS SP8 confocal microscope.

Brain immunofluorescence

For neuronal activation analysis, hypothalamic slices containing PVN and ARC nuclei were extensively washed in 0.1% Triton X-100 KPBS buffer and blocked in 2% goat anti-serum in KPBS plus 0.1% Triton X-100. Sections were incubated with rabbit anti-c-FOS antibody (1:200, Cell Signaling) in blocking buffer for 1 h at room temperature. After washing with KPBS, slices were incubated with anti-rabbit Alexa Fluor 647 antibody (1:1000; Invitrogen) for 1 h at room temperature, followed by counterstaining with Hoechst 3328 for nuclear staining (1 mg/mL, Sigma-Aldrich). For the analysis of fluorescein in brain slices, immunostaining of brain cells was performed using antibodies against neurons (rabbit anti-NeuN, 1:500, Abcam; rabbit anti-NSE, 1:250, Abcam), astrocytes (rabbit anti-GFAP, 1:1000, Invitrogen) and microglia (rabbit anti-Iba1, 1:500, WAKO) in blocking buffer for 1h at room temperature, followed by incubation with the secondary antibody (Alexa Fluor 647) and Hoechst, as described above. After immunostaining, slices were mounted into Superfrost Plus Slides (Thermo Fisher) using antifade Fluoromount-G® (Southern Biotech) and coverslips. Images were taken using a Leica TCS SP8 confocal microscope equipped with a 20x and 40x objective. Fluorescence integrated density after image masking was calculated using ImageJ FIJI (NIH) software.

RNA extraction and RT-PCR

Total RNA was extracted from liver and BAT using Trizol Reagent (Fisher Scientific, Madrid, Spain). Retrotranscription and quantitative RT-PCR (qPCR) were performed as previously described [3]. SYBR Green or Taqman Gene Expression assay primers used in the study (IDT DNA Technologies, Leuven, Belgium) are detailed in Table S2. Relative mRNA levels were measured using the CFX96 Real-time System, C1000 Thermal Cycler (BioRad). Relative gene expression was estimated using the comparative Ct ($2^{-\Delta\Delta ct}$) method and normalized to *Hprt/Gapdh*.

Table S1. Summary of size and polydispersity of the different micelles used. Preparation and size measurements were performed in triplicate (n = 3) and indicate mean ± s.d. except for [#], which was only prepared once (n = 1).

Cargo	**Micelle type**	**Polymer/s used**	**Size (nm)**	**Polydispersity**
(±)-C75-CoA	Non-crosslinked	PEG-PAsp(Aldehyde)-PLys	44.0 ± 0.28	0.13 ± 0.009
(±)-C75-CoA	Crosslinked	PEG-PAsp(Aldehyde)-PLys	43.1 ± 0.26	0.12 ± 0.013
(±)-C75-CoA	Non-crosslinked	PEG-PLys	41.4 ± 0.68	0.12 ± 0.019
(±)-C75-CoA	Crosslinked (FRET)	PEG-PAsp(Aldehyde)-PLys-Fluorescein	60.6 ± 3.58	0.14 ± 0.008
Fluor-CoA [#]	Non-crosslinked	PEG-PAsp(Aldehyde)-PLys	53.2	0.10
Fluor-CoA	Crosslinked	PEG-PAsp(Aldehyde)-PLys	43.9 ± 0.40	0.08 ± 0.006

Table S2. List of the primers used for the RT-PCR assays in hypothalamus, liver or adipose tissue.

SYBR Green primers		
Gene	**Direction**	**Sequence**
AgRP	For	5'-TTTGTCCTCTGAAGCTGTATGC
	Rev	5'- GCATGAGGTGCCTCCCTA
NPY	For	5'-TCCGCTCTGCGACACTACAT
	Rev	5'-TGCTTTCCTTCATTAAGAGGT
POMC	For	5'-TGAACATCTTTGTCCCCAGAG
	Rev	5'-TGCAGAGGCAAACAAGATTGG
PGC1-α	For	5'- GAAAGGGCCAAACAGAGAGA
	Rev	5'- GTAAATCACACGGCGCTCTT
CIDEA	For	5'-GCCTGCAGGAACTTATCAGC
	Rev	5'-AGAACTCCTCTGTGTCCACCA
PRDM16	For	5'-CCTAAGGTGTGCCCAGCA
	Rev	5'-CACCTTCCGCTTTTCTACCC
PEPCK	For	5'-CCACAGGCACTAGGGAAGGC
	Rev	5'-GGCGGAGCATATGCTGATCC
G6Pase	For	5'-TCAACCTCGTCTTCAAGTGGATT
	Rev	5'-CTGCTTTATTATAGGCACGGAGCT
PKLR	For	5'-AGATGCAACATGCGATTGCC
	Rev	5'-GCACAGCACTTGAAGGAAGC
CPT1A	For	5'-GACTCCGCTCGCTCATTC
	Rev	5'-AAGGCCACAGCTTGGTGA
HPRT	For	5'-GGACCTCTCGAAGTGTTGGATAC
	Rev	5'-GCTCATCTTAGGCTTTGTATTTGGCT
GAPDH	For	5'-TCCACTTTGCCACTGCA
	Rev	5'-GAGACGGCCGCATCTTCTT
TaqMan probes		
Gene	**Reference**	**Dye**
UCP-1	Mm.PT.58.7088262	Hex
GAPDH	Mm.PT.39a.1	Fam

Fig. S1. Transmission electron microscopy (TEM) images. (A) (±)-C75-CoA loaded Crosslinked micelle (B) (±)-C75-CoA loaded Non-crosslinked micelle (C) Mixture of PEG-PAsp(Aldehyde)-PLys and PEG-PAsp(Hydrazide) polymers in 10 mM phosphate buffer pH 7.4 . Scale bar 50 nm.

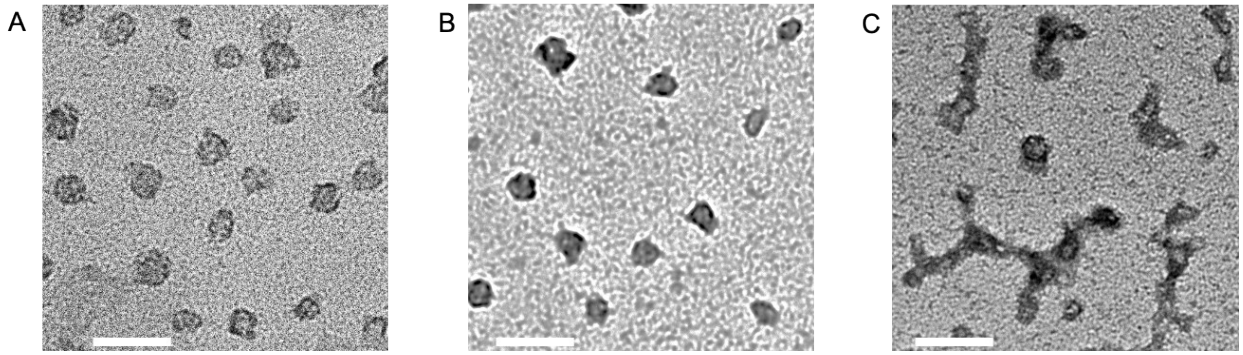

Fig. S2. Size profile and dissociation of non-crosslinked polymeric micelles (PM). (A) Size profile of non-crosslinked (±)-C75-CoA diblock PM. (B) Effect of dextran sulfate sodium (DSS) on scattered light intensity of diblock PM. Data are expressed as mean ± SEM (n=3-4).

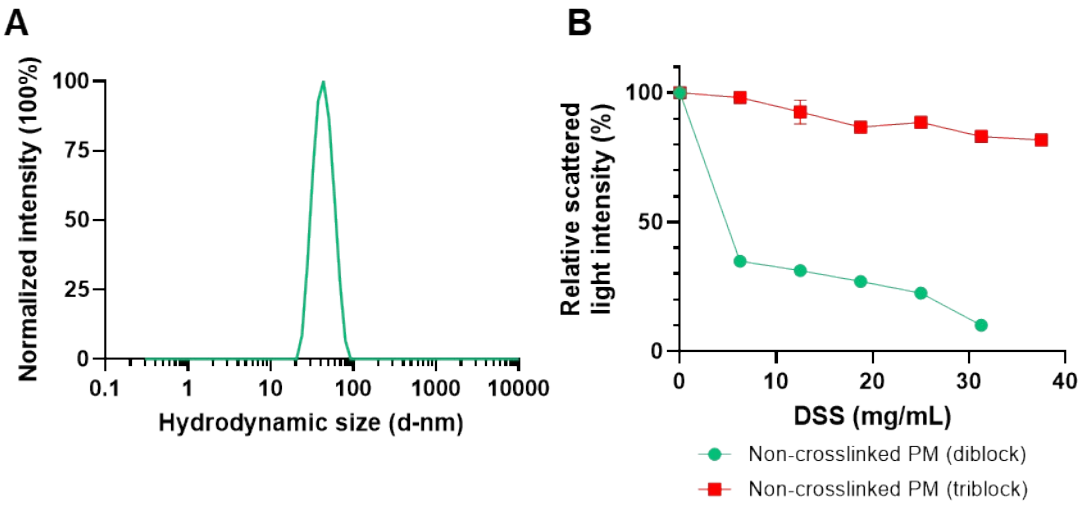

Fig. S3. Encapsulation efficiency of non-crosslinked and crosslinked micelles in response to phosphate buffer (PB) and artificial cerebrospinal fluid (aCSF). Data expressed as mean ± SEM (n=3-4) were compared using one-way ANOVA with Tukey's post-hoc test, ***p<0.001.

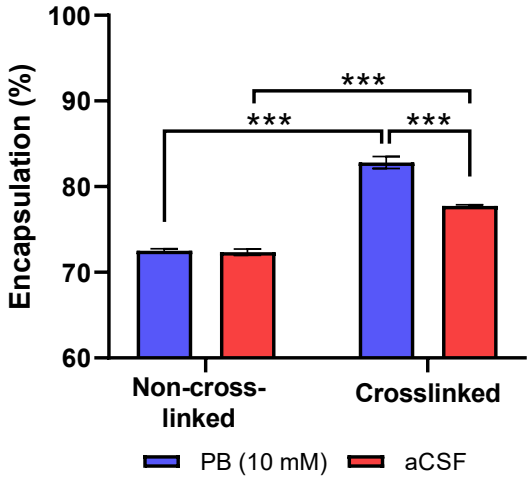

Fig. S4. Size profile, encapsulation and release of Fluor-CoA polymeric micelles (PM). (A) Size profile of Fluor-CoA PM. (B) Encapsulation of Fluor-CoA PM. (C) Release of Fluor-CoA PM in cell medium at 4ºC or 37ºC. (D) Release of the cargo in PBS or artificial cerebrospinal fluid (aCSF) at 37 ºC. Data are expressed as mean ± SEM (n=3-4), compared using one-way ANOVA with Tukey's post-hoc test, *p<0.05, **p<0.01, ***p<0.001.

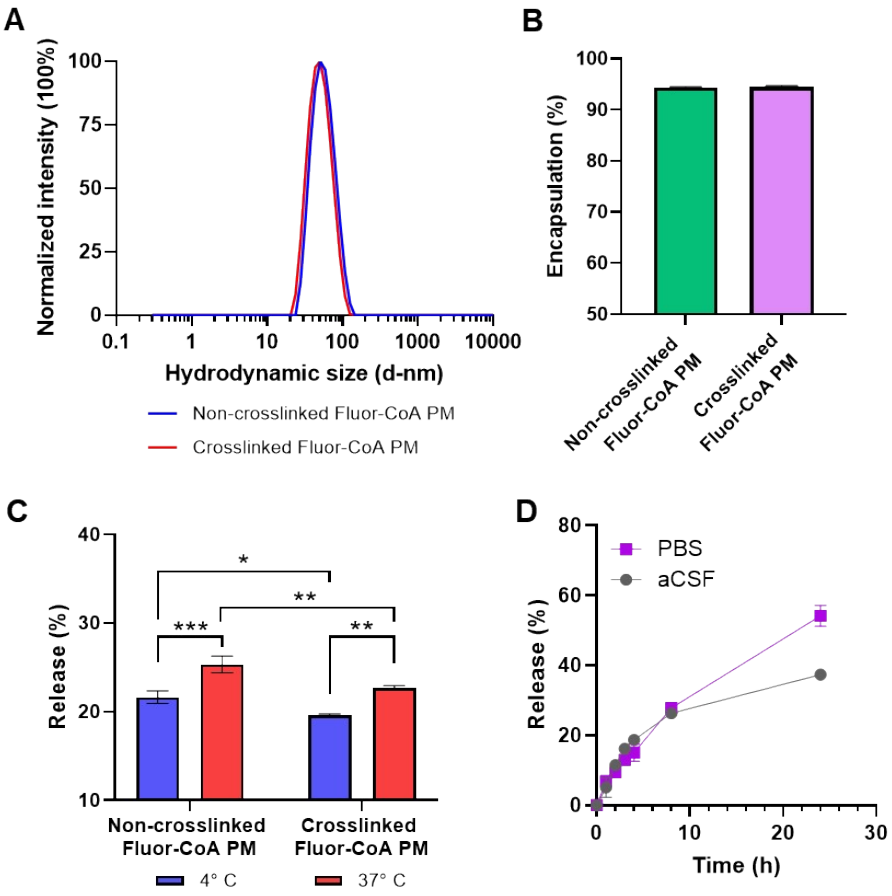

Fig. S5. Fluorescent localization of the fluorescent tracer of the micelle with endolysosomes and mitochondria. Representative images of GT1-7 neurons indicating endolysosomes (LysoTracker; red), mitochondria (MitoTracker; red), nuclei (blue) and the fluorescent cargo of the nanomedicine (Fluorescein, green) after 1 hour of treatment. Scale bar = 10μm.

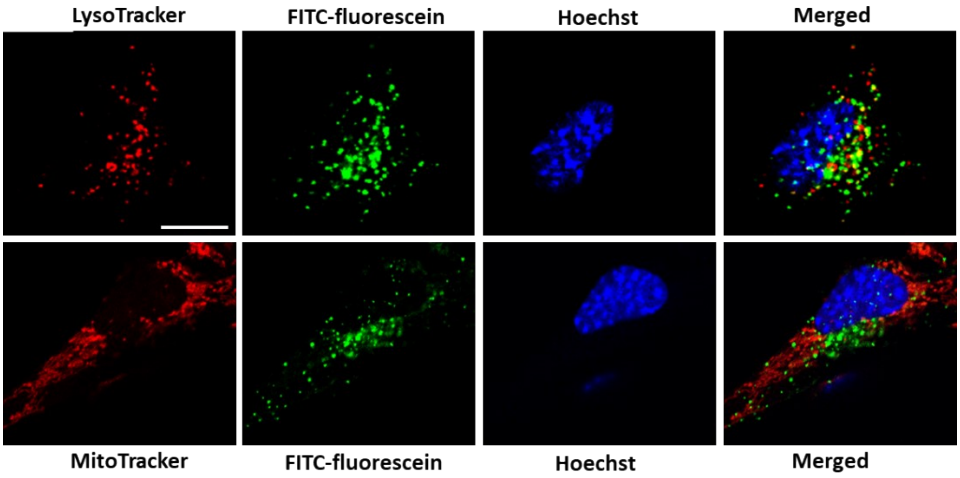

Fig. S6. Fluorescent tracer of the nanomedicine reaches the hypothalamus. Representative images of the main hypothalamic regions related to the regulation of food intake and energy expenditure, arcuate (ARC), ventromedial (VMH) and paraventricular hypothalamus (PVN), after 1 hour of ICV infusion of the nanomedicine. Scale bar = 50µm. The fluorescent tracer fluorescein is indicated in green (FITC).

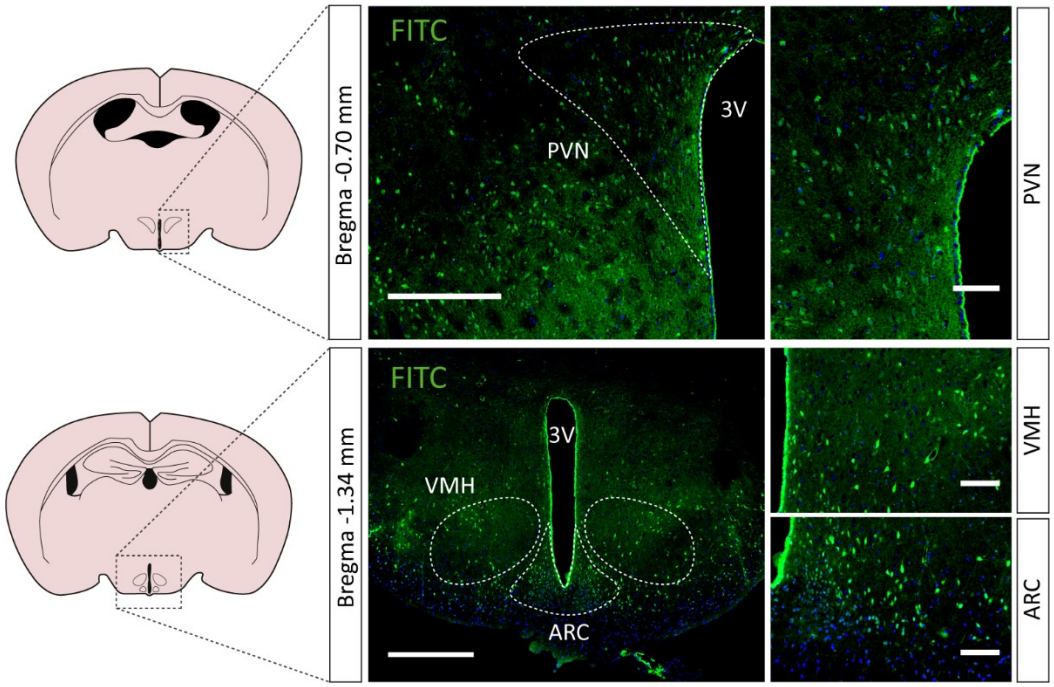

Fig. S7. Analysis of microglia activation in hypothalamus. Iba-1 expression at arcuate (ARC) and paraventricular (PVN) nucleus of the hypothalamus after 2 hours of treatment. (A) Vehicle, free cargo (fluorescein-CoA) and nanomedicine Iba-1 positive cells in ARC. (B) Quantification of the number of Iba-1 positive cells per ARC section. (C) Vehicle, free cargo (fluorescein-CoA) and nanomedicine Iba-1 positive cells in PVN. (D) Quantification of the number of Iba-1 positive cells per PVN section. All values are expressed in mean ± SD (n=3, 2 slice/animal). Scale bar = 50µm; magnification 40X. In (B, D) ns>0.05, using one-way ANOVA with Tukey's multiple comparison tests as post-hoc analysis. Iba-1 is indicated in red and nuclei in blue.

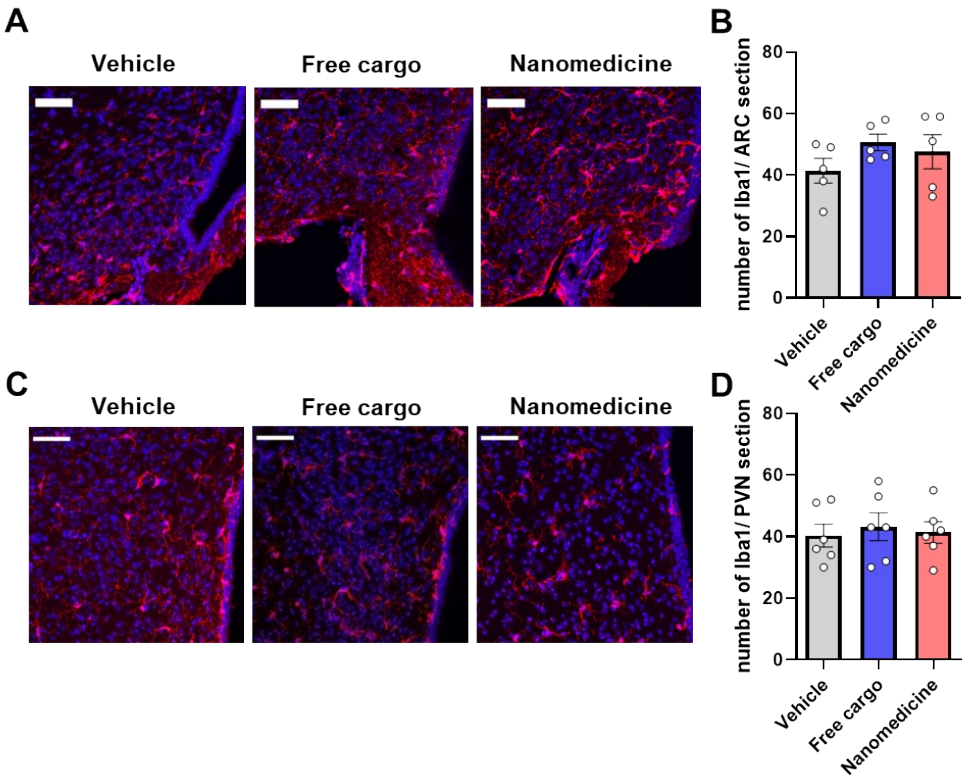

Fig. S8. Characterization of the triblock polymer. (A) ^{1}H NMR spectrum (400MHz, D_2O, 25°C) of the *PEG–PAsp–PLys* triblock polymer with gel chromatogram as an insert. (B) ^{1}H NMR spectrum (400MHz, DMSO-*d6*, 80 °C) of the *PEG-PAsp(Aldehyde)-PLys-TFA* triblock polymer.

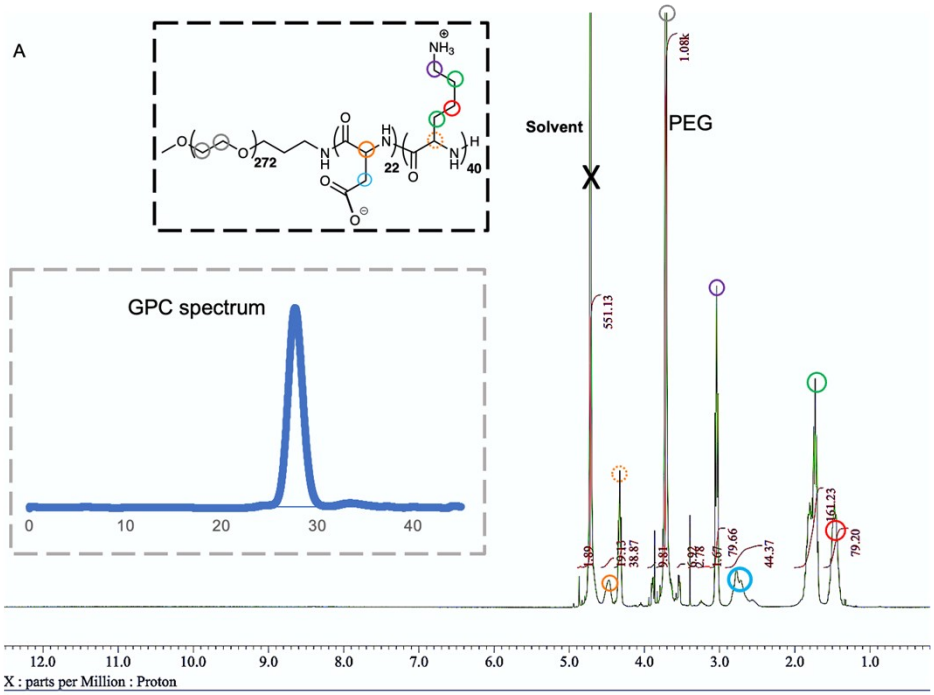

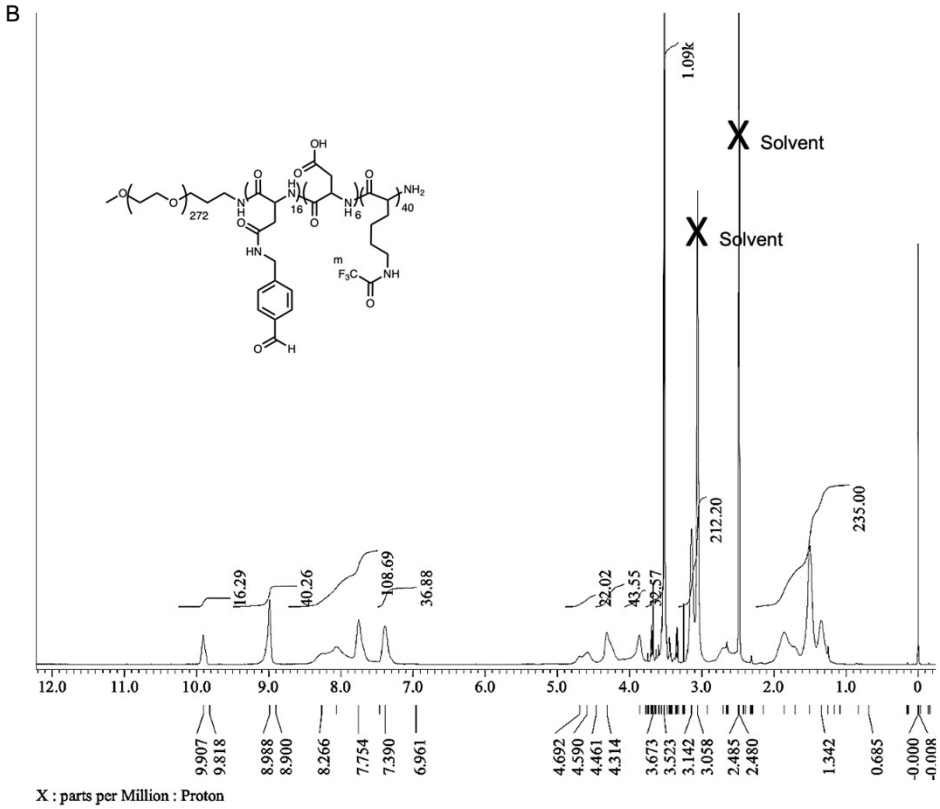

References:

1 S. Quader, H. Cabral, Y. Mochida, T. Ishii, X. Liu, K. Toh, H. Kinoh, Y. Miura, N. Nishiyama and K. Kataoka, *J. Control. Release*, 2014, **188**, 67–77.

2 W. K. D. Paraiso, J. Garcia-Chica, X. Ariza, S. Zagmutt, S. Fukushima, J. Garcia, Y. Mochida, D. Serra, L. Herrero, H. Kinoh, N. Casals, K. Kataoka, R. Rodríguez-Rodríguez and S. Quader, *Biomater. Sci.*, 2021, **9**, 7076–7091.

3 R. Rodríguez-Rodríguez, C. Miralpeix, A. Fosch, M. Pozo, M. Calderón-Domínguez, X. Perpinyà, M. Vellvehí, M. López, L. Herrero, D. Serra and N. Casals, *Mol. Metab.*, 2019, **19**, 75–85.